Biochimica et Biophysica Acta 1797 (2010) 641–648

Contents lists available at ScienceDirect

Biochimica et Biophysica Acta

journal homepage: www.elsevier.com/locate/bbabio

The flitting of electrons in complex I: A stochastic approach

Stéphane Ransac [a,b], Clément Arnarez [c], Jean-Pierre Mazat [a,b,*]

[a] Université de Bordeaux 2, 146 rue Léo-Saignat, F 33076, Bordeaux-cedex, France
[b] Mitochondrial physiopathology laboratory, INSERM U688, Bordeaux, France
[c] CBMN – UMR 5248, 2 rue R. Escarpit, 33600 Pessac, France

ARTICLE INFO

Article history:
Received 24 October 2009
Received in revised form 19 February 2010
Accepted 6 March 2010
Available online 15 March 2010

Keywords:
Gillespie algorithm
Complex I
Stochastic modelling

ABSTRACT

A stochastic approach based on the Gillespie algorithm is particularly well adapted to describe the time course of the redox reactions that occur inside the respiratory chain complexes because they involve the motion of single electrons between the individual unique redox centres of a given complex. We use this approach to describe the molecular functioning of the peripheral arm of complex I based on its known crystallographic structure and the rate constants of electron tunnelling derived from the Moser and Dutton phenomenological equations. There are several possible electrons pathways but we show that most of them take the route defined by the successive sites and redox centres: $NADH^+$ site – FMN – N3 – N1b – N4 – N5 – N6a – N6b – N2 – Q site. However, the electrons do not go directly from NADH towards the ubiquinone molecule. They frequently jump back and forth between neighbouring redox centres with the result that the net flux of electrons through complex I (i.e. net number of electrons reducing a ubiquinone) is far smaller than the number of redox reactions which actually occur. While most of the redox centres are reduced in our simulations the degree of reduction can vary according to the individual midpoint potentials. The high turnover number observed in our simulation seems to indicate that, in the whole complex I, one or several slower step(s) follow(s) the redox reactions involved in the peripheral arm. It also appears that the residence time of FMNH• and SQ• (possible producers of ROS) is low (around 4% and between 1.6% and 5% respectively according to the values of the midpoint potentials). We did not find any evidence for a role of N7 which remains mainly reduced in our simulations. The role of N1a is complex and depends upon its midpoint potential. In all cases its presence slightly decreases the life time of the flavosemiquinone species. These simulations demonstrate the interest of this type of model which links the molecular physico-chemistry of the individual redox reactions to the more global level of the reaction, as is observed experimentally.

1. Introduction

NADH:ubiquinone oxidoreductase, also called respiratory complex I, is the first component of the respiratory chain of most eukaryotes and many bacteria [1–5]. It couples the electron transfer between NADH and ubiquinone to proton translocation across the inner membrane of the organelle [1–9].

The difficulties in characterizing complex I arise from the fact that it is a huge complex of proteins and other molecules, with a molecular mass of about 1 MDa. At least 45 polypeptide subunits with a dual genetic origin have been identified as constituents of the mammalian complex I [10]. Most of them are encoded by nuclear genes, are synthesized in the cytoplasm and imported into the mitochondria. Some of the subunits – seven in humans – are hydrophobic proteins encoded by mitochondrial DNA [11]. The function of complex I is to transfer electrons from NADH to ubiquinone through a number of protein-bound prosthetic groups: one FMN and up to nine iron–sulphur (Fe/S) clusters depending on the species [1–3,6–8]. In addition, two or three ubisemiquinone radicals have been identified as obligatory intermediates of the reaction [8,12–14]. This electron transfer reaction is coupled to the translocation of protons across the inner mitochondrial membrane according to the reaction:

$$NADH + H^+ + Q + 4\ H^+_{matrix} <=> NAD^+ + QH_2 + 4\ H^+_{intermembrane\ space}.$$

This reaction helps to maintain the proton-motive force that eventually results in ATP synthesis [1,15]. In the presence of a proton-motive force, the reaction can be reversed. Bacteria like *Escherichia coli* and *Paracoccus denitrificans* contain proton-pumping enzymes equivalents to mitochondrial complex I, also named NDH1 [16,17]. Enzymes equivalent to mitochondrial complex I have also been identified in chloroplasts [2] and more recently in archaea [18]. Structurally, complex I involves two major domains, one consisting of a peripheral arm with the hydrophilic proteins located in the aqueous milieu and the other consisting of a membrane arm with the hydrophobic proteins being buried in the lipid bilayer [19–22]. They

* Corresponding author. Inserm U688 Université de Bordeaux 2, 146 rue Léo-Saignat, F 33076, Bordeaux-cedex France. Tel.: +33 557 571 506.
E-mail address: jpm@u-bordeaux2.fr (J.-P. Mazat).

0005-2728/$ – see front matter © 2010 Published by Elsevier B.V.
doi:10.1016/j.bbabio.2010.03.011

are arranged perpendicularly to each other in the form of an L. The membrane arm is mainly embedded in the mitochondrial inner membrane, while the majority of the peripheral arm is located in the matrix [23]. Each arm is assembled independently of the other and then the two arms are joined together [24]. The peripheral arm contains most, if not all, prosthetic groups of complex I (Fig. 1) and is thus responsible for the electron transfer reactions. The membrane arm is thought to play a role in proton translocation [25].

The relative positions of the binding sites and redox centres are known in detail from the X-ray structure of the peripheral arm of the bacterial complex from *Thermus thermophilus* [26,27].

It has been hypothesized that one electron is transferred to the tetranuclear Fe/S cluster N3 from the flavine mononucleotide (FMN) close to the NADH binding site (Fig. 1), while the second electron is temporarily "stored" on the binuclear cluster N1a [26,28]. The electron on cluster N3 is transferred to the acceptor quinone via a chain composed of the binuclear cluster N1b and the tetranuclear clusters N4 and N5, N6a and N6b, and N2 [8,29–34]. After reoxidation of N3 by the electron transfer chain, the electron stored on N1a, which is located 11 Å away from the FMN, could move back to the FMN and undergo the same fate as the first electron. It has been proposed that this mechanism reduces the probability of producing superoxide radicals at the flavin in its semiquinone state [26]. In addition to these Fe/S clusters obviously involved in electron transfer, the tetranuclear Fe/S cluster N7 has been identified in the structure [26,27]. Cluster N7 does not seem to participate in the physiological electron transfer reaction. Nevertheless, it can be chemically reduced by dithionite [35].

To better understand the mechanism of the electron transfer and the role of the different clusters in the peripheral arm of complex I, we used a stochastic approach based on the known spatial structure of this peripheral arm and the kinetic parameters described by Moser et al. [36] as already done for bc_1 complex [37]. Because we were interested only in the electron transfer in the peripheral arm, which is located outside the mitochondrial membrane, we did not take into account the membrane potential and the proton transfers.

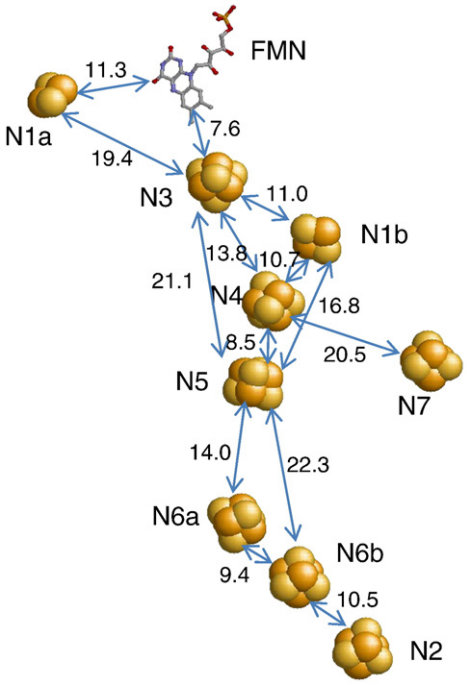

Fig. 1. Organization of the redox centres in Complex I according to [26]. Edge-to-edge distances are in Å. The distance between the quinone binding site and N2 (12 Å) is given centre to centre [58]. NADH is close to FMN (3.2 Å) [27].

2. Methods/model

A critical step in our model is the calculation of the rate constants of electron transfers between the redox centres. To this end, we used the equation formulated by Moser et al. [36,38,39]:

$$\log k_{et}^{exer} = 15 - 0.6D - 3.1\frac{(\Delta G^o + \lambda)^2}{\lambda}. \quad (1)$$

For exergonic reactions ($\Delta G°<0$), k_{et}^{exer} (exer means exergonic) is a function of the distance D between the redox centres (edge to edge in Å) and of the driving force ΔG^o (in eV). The parameter λ is the reorganization energy. Unfortunately, the latter parameter is not known so we used the value of $\lambda = 0.7$ eV proposed by Moser et al. [36,38,39] on an empirical basis.

Since the reverse reaction is possible, we also had to estimate the endergonic reaction (indicated by the superscript "ender") which is calculated according to Moser et al. [38] as shown in Eq. (2). This equation simply expresses the equilibrium constant (K) of the electron transfer, as demonstrated in Eq. (3) done at a temperature of 30 °C.

$$log k_{et}^{ender} = 15 - 0.6D - 3.1\frac{(\Delta G^o + \lambda)^2}{\lambda} + \frac{\Delta G^o}{0.06} \quad (2)$$

$$K = \frac{k_{et}^{ender}}{k_{et}^{ender}} = e^{-\frac{\Delta G^o}{kT}} => \log k_{et}^{ender} = \log k_{et}^{exer} + \frac{\Delta G^o}{0.06}. \quad (3)$$

To calculate the electron tunnelling rates, we thus need to know ΔG^o and the distance D between redox centres. The ΔG^o values shown in Table 2 are calculated from the midpoint redox potentials listed in Table 1 (see also (Fig. 2). We measured the distances edge to edge between the redox centres and the binding sites of complex I structure of *Thermus thermophilus* [26,27] which is the only known structure of the hydrophilic domain of respiratory complex I. Then we calculated the electron tunnelling rate constants (Table 2). Fig. 1 summarizes the redox centres of complex I with FMN and the distances used for our simulation. Because the rate constants decrease rapidly with the distance D according to Eqs. (1) and (2), only transfer reactions between redox centres shorter than 22 Å are considered in our model, i.e. 19 electron (reversible) transfer reactions.

As already mentioned, the distances are measured on *Thermus thermophilus* structure of complex I which uses menaquinone as electron acceptor. However the midpoint potentials of complex I centres are not known in this organism. In order to overcome this lack of data, we used two sets of midpoint potentials for equivalent redox

Table 1
Single-electron redox centre midpoint potentials in complex I according to [34] (parameter set #1) and to [38] (parameter set #2). In each parameter set, some values are missing. The corresponding values used for our simulations are indicated in italic.

Redox couple	Parameter set #1 E° (in eV) from [34]	Parameter set #2 E° (in eV) from [38]
NADH/NAD+	−0.32	−0.32
FMNH2/FMNH•	−0.293	*−0.293*
FMNH•/FMN	−0.389	*−0.389*
QH2/SQ•	0	*0*
SQ•/Q	−0.12	*−0.12*
N1a	−0.38	−0.235
N1b	−0.25	−0.282
N2	−0.10	−0.250
N3	−0.25	−0.315 (N7?)
N4	−0.25	−0.330 (N5?)
N5	−0.25	−0.330 (N4?)
N6a	−0.25	*−0.275*
N6b	−0.25	−0.275
N7	*−0.25*	−0.315 (N3?)

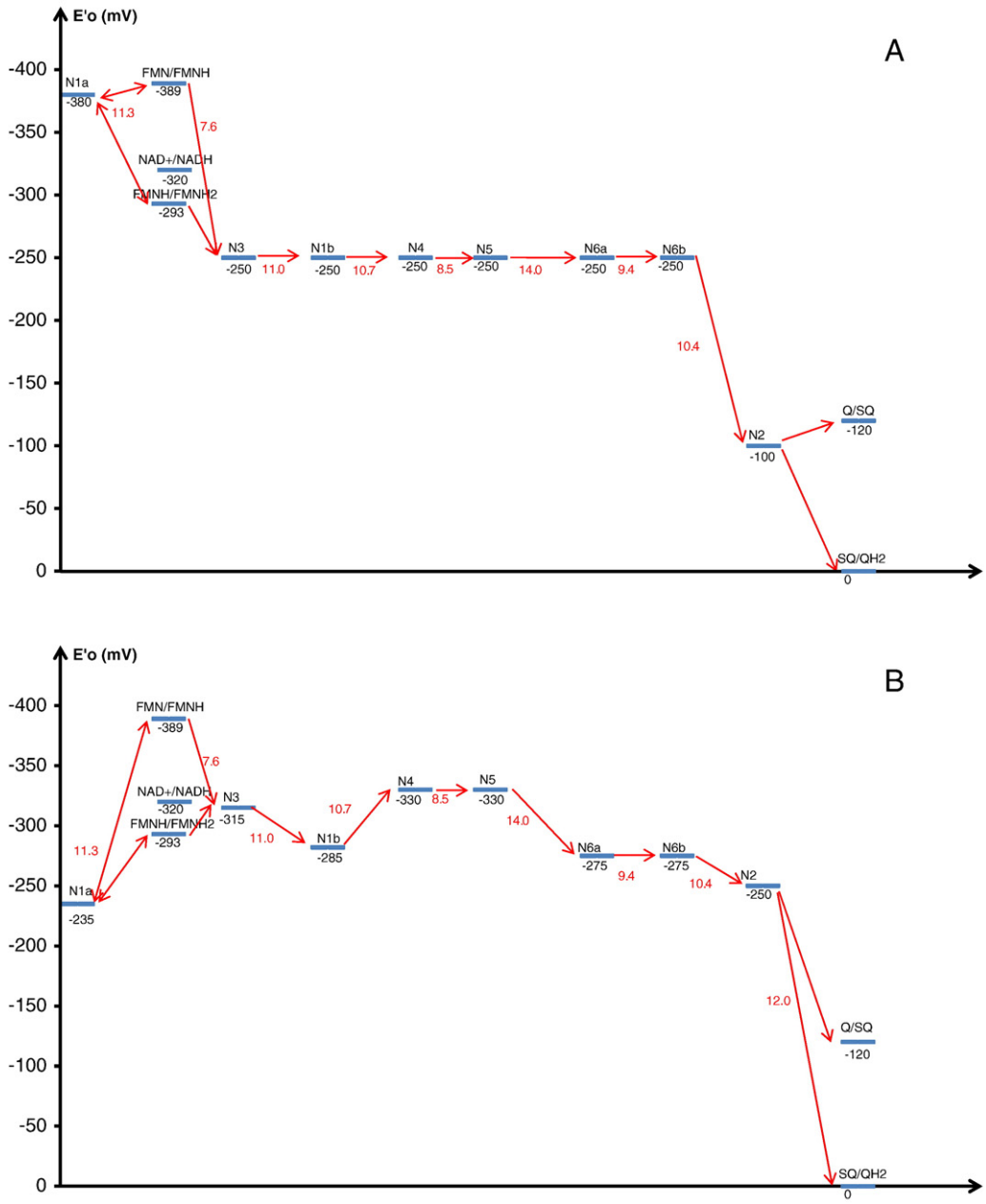

Fig. 2. Energetics of the electrons transfers in the model. A, graphical representation of data listed in Table 1 (parameter set #1). B, graphical representation of parameter set #2 from Table 1. Values for NADH, flavinmononucleotide and quinone are those of parameter set #1. Distances in red.

centres reported in bovine heart, set #1 [8,29,40] (Fig. 2A) and in *E. coli*, set #2 [41] (Fig. 2B) (see also Table 1). Since these organisms use ubiquinone as electron acceptors we take in our simulation the midpoint potential of ubiquinone (as in [29]) and not of menaquinone.

Furthermore the assignation of the E^o measurement to iron–sulphur clusters N_4 and N_5 was recently challenged [31,42]. As demonstrated in the following, because the ΔG^o of these iron–sulphur centres are close to each other, this possible discrepancy, if any, has little effect on our simulation.

In our model we also need the rate constants for substrates (NADH, Q, SQ•), and products (NAD^+, SQ•, QH_2) binding and release. These values are unknown and we had to estimate them. Our choice was guided by the following considerations: (i) to have values that correspond to a good binding of the substrates and a good release of the products, (ii) to have ratios of the binding over release rate constants corresponding to the known or estimated K_d values, (iii) to obtain the known K_M and K_i values. It is indeed possible to simulate the *in vitro* kinetics in the same manner as they are recorded with a spectrophotometer; with these kinetics *in silico* it is possible to calculate the K_M for substrates and the K_i for products which correspond to the set of rate constants used, and to adjust these latter values in order to obtain the known K_M and K_i values [43].

In the model the substrates and products concentrations are maintained constant to mimic the rest of the Q metabolism (QH_2 <=> Q due to complex III, complex II, etc.) and the mitochondrial metabolism (NAD^+ <=> NADH). In this case, we obtain a kind of steady-state characterized by a constant rate of Q reduction and NADH oxidation (see Fig. 3).

For the simulation we used only one complex I molecule. From the point of view of the reactions that occur inside complex I, it is equivalent in a stochastic process to consider, on average, the reactions of n independent molecules during a time Δt or the functioning of a single molecule during the time $n \cdot \Delta t$, provided that the ratios of the products and substrates to complex I remain the same.

Table 2
The distances between redox centres are from the 3D structures [25]. ΔG^0 are calculated from the E_0 values in table I (parameters set #1). k_f (forward reaction) and k_b (backward reaction) are calculated as explained in the model section. Binding constants are chosen as indicated in the model section. QH_2, SQ• and Q mean ubiquinol, semiubiquinone and ubiquinone respectively.

Reactions	Distance (in Å)	ΔG° (in eV)	$k_{forward}$ (in s^{-1})	$k_{backward}$ (in s^{-1})
e^- transfer from NADH to FMN	3.2	0.02	$1.44\ 10^{12}$	$3.10\ 10^{12}$
e^- transfer from FMNH2 to N1a	11.3	0.087	$2.13\ 10^{5}$	$5.99\ 10^{6}$
e^- transfer from FMNH• to N1a	11.3	−0.009	$2.12\ 10^{6}$	$1.50\ 10^{6}$
e^- transfer from FMNH2 to N3	7.6	−0.043	$5.25\ 10^{8}$	$1.01\ 10^{8}$
e^- transfer from FMNH• to N3	7.6	−0.139	$1.73\ 10^{9}$	$8.35\ 10^{6}$
e^- transfer from N3 to N1b	11.0	0	$2.81\ 10^{6}$	$2.81\ 10^{6}$
e^- transfer from N3 to N4	13.8	0	$6.19\ 10^{4}$	$6.19\ 10^{4}$
e^- transfer from N1b to N4	10.7	0	$4.23\ 10^{6}$	$4.23\ 10^{6}$
e^- transfer from N1b to N5	16.8	0	$1.04\ 10^{3}$	$1.04\ 10^{3}$
e^- transfer from N4 to N5	8.5	0	$8.50\ 10^{7}$	$8.50\ 10^{7}$
e^- transfer from N5 to N6a	14.0	0	$4.71\ 10^{4}$	$4.71\ 10^{4}$
e^- transfer from N6a to N6b	9.4	0	$2.49\ 10^{7}$	$2.49\ 10^{7}$
e^- transfer from N6b to N2	10.4	−0.15	$4.31\ 10^{7}$	$1.36\ 10^{5}$
e^- transfer from N1a to N3	19.4	−0.13	161	1.10
e^- transfer from N4 to N7	20.4	0	7.66	7.66
e^- transfer from N3 to N5	21.1	0	2.95	2.95
e^- transfer from N5 to N6b	22.3	0	0.575	0.575
e^- transfer from N2 to Q	12	0.02	$4.43\ 10^{5}$	$9.54\ 10^{5}$
e^- transfer from N2 to SQ•	12	−0.10	$2.71\ 10^{6}$	$5.84\ 10^{4}$
NADH binding			$4.0\ 10^{8}\ M^{-1}$	100
NAD^+ binding			$1.0\ 10^{7}\ M^{-1}$	1000
Q binding			$4.0\ 10^{7}\ M^{-1}$	100
SQ• binding			$2.0\ 10^{7}\ M^{-1}$	100
QH_2 binding			$2.0\ 10^{7}\ M^{-1}$	1000

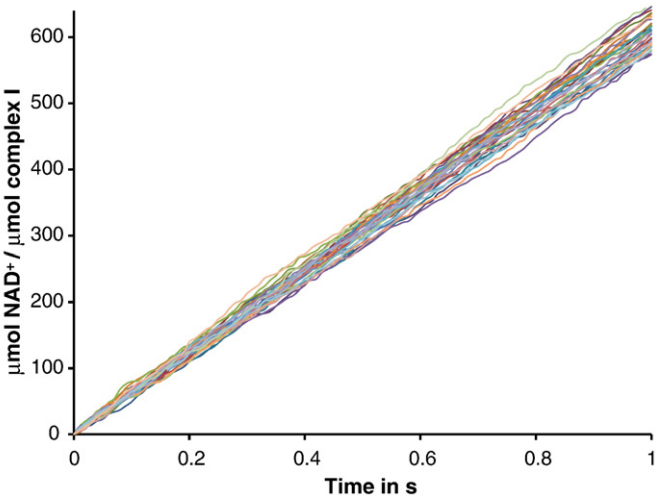

Fig. 3. Recording of newly formed NAD^+ in 30 simulations done with a single complex I at steady state as a function of time with parameter set #1. The number of substrates and products is kept constant ([Q] = [QH_2] = 20, [NADH] = 2, [NAD^+] = 15 and complex I = 1 molecule(s)).

During the simulation, the number of electron transfers through each redox reaction can be measured.

The stochastic analysis of enzymatic reactions involves measuring numbers of molecules. Concentrations thus have to be converted into numbers of molecules, which requires knowing the average volume of the mitochondrial membrane and mitochondrial matrix accessible to one molecule of complex I. Traditionally the matrix volume is taken as being equal to 1 µL/mg prot (prot means mitochondrial proteins) [44,45]. Although we did not measure the content in complex I, it now appears that most of complex I is involved in a supercomplex assembly in the ratio of 1:2 monomer of complex III [46]. In rat muscle, Benard et al. [47] measured a concentration of 121 pmol of complex III monomer per mg of protein. This means 60 pmol of complex I/mg prot. by applying the above-mentioned hypothesis. This value is close to the value of 100 pmol/mg protein found with piericidin titration [48]. Assuming that the inner membrane volume is of the order of half of the matrix volume, i.e. 0.5 µL/mg prot., this gives a concentration of 120 pmol/µL of complex I in the membrane, which means 120 µmol/L. Taking into account the Avogadro number we calculated a total number of 720 10^{17} molecules/L (of membrane). By taking the inverse of this value we obtain a volume of 1.4 10^{-20} L of membrane/molecule of Complex I and thus of 2.8 10^{-20} L of matrix possibly available for one molecule of complex I.

In the same paper, Benard et al. [47] gave the total content in coenzyme Q: 2348 pmol/mg prot. This means a ratio Q:Complex III monomer of 19.4 and thus a ratio of 39 per dimer of complex III, i.e. per complex I. In our simulations, we took 20 molecules of Q and 20 molecules of QH_2 per molecule of complex I (corresponding to a membrane concentration of 2.4 mM).

The concentrations [NADH] = 0.13 mM and [NAD^+] = 0.9 mM are taken from the literature [49,50], which corresponds to 2 molecules of NADH and 15 molecules of NAD^+ in the matrix volume surrounding a single complex I. We would like to stress that these calculations do not aim to give exact values but only to give an order of magnitude of the number of molecules of substrates and products associated with one molecule of complex I.

The Gillespie algorithm [51] defines two random processes: a) the random choice of a reaction from amongst all possible reactions at a given time and b) the random time at which this reaction occurs, once a reaction is chosen. The calculation of the corresponding probabilities is based on the evaluation of the following parameters: for each reaction R_μ ($\mu = 1$ to 26), we calculate h_μ, the number of distinct possible molecular reactant combinations. h_μ are calculated from the quantity (most of the time 0 or 1 except for the free substrates and products) of each redox centre or molecule present at each stochastic step. According to the Gillespie model we can equate the stochastic reaction constant c_μ to the electron tunnelling rate constant $c_\mu = k_\mu$. However, since two molecules have to interact for the binding reaction to occur, the stochastic reaction constant is equal, in this case, to the binding rate constant divided by the reaction volume. These volumes represent the part of the matrix or membrane surrounding one molecule of complex I and are estimated by the mitochondrial volumes and the number of complex I molecules per mitochondria as described above. Using these stochastic reaction constants c_μ and the number of distinct molecular reactant combinations h_μ, we calculate $a_\mu = h_\mu \cdot c_\mu$ which gives the probability a_μ/a_0 ($a_0 = \Sigma a_\mu$) that the reaction R_μ occurs at a given step. All these parameters are updated after each stochastic reaction in order to take into account the changes in redox status or bound species. The reaction R_μ is chosen using a random number in the unit interval multiplied by a_0 [51]. The reaction time interval between two reactions is given by $\Delta t = 1/(a_0) \cdot \ln(1/r)$ where r is a random number between 0 and 1, according to an exponential law of probability with parameter a_0 [51]. The whole process can be summarized in the short algorithm compiled as a Fortran program:

Initialization of the number of species /. Computation of h_μ and then of a_μ values /. First random number in the interval [0; a_0] => Choice of the reaction /. Second random number => Computation of the Δt of the chosen reaction /. $t_{n+1} = t_n + \Delta t$ /. Update of the new species number / If n + 1 = N; End; if not the process is repeated /. End.

In our first simulations nearly all the reaction steps were used by rapid exchanges of electrons between reduced NADH and FMN since these molecules are very close to each other (3.2 Å). To avoid wasting stochastic steps, we considered the reaction at equilibrium. We checked whether introducing such a rapid equilibrium does not change the global results which can be obtained with the initial model for a much greater number of stochastic steps.

3. Results and discussion

Fig. 3 shows the superposition of 30 simulations where complex I functions at steady state i.e. coupled to an oxidation of UQH_2 and reduction of NAD^+. In these conditions the number of substrates and products molecules are constants: 20 molecules of UQ and UQH_2 which corresponds to 2.4 mM and 2 molecules of $NADH^+$ and 15 molecules of NAD, which in turn correspond to 0.13 and 0.9 mM respectively for a unique molecule of complexe I. The mean observed rate in these conditions (parameter set #1) is $609 \pm 21\ s^{-1}$. In the absence of products and with saturating substrate concentrations, we measure a k_{cat} of $842\ s^{-1}$ (see Table 5). This value is not too far away from the value of $600\ s^{-1}$ reported in *E. coli* [52], but not very close to the value of 150–200 s^{-1} in beef heart [53]. These values are however much lower than the maximal turnover $21{,}539\ s^{-1}$ which can be derived from the value of the rate constants of the individual steps assuming that all electrons go directly from the NADH to the Q site without returning. This large difference with the observed turnover is essentially due to the huge number of electron exchanges between the redox centres, as shown in Table 3 where we followed the fate of the electrons of 6055 NADH molecules bound to the molecule of complex I. The first column in the table indicates the number of times a centre was reduced (i.e. received an electron). These numbers include many electrons transfers to and fro. However, what actually matters here is the number of electrons going through each redox centre and participating effectively in the global reaction. These numbers are shown in column 2 of Table 3 in which we exclude the to and fro reactions. The 6055 NADH molecules give 12,110 electrons which circulate in complex I towards the reduction of 6050 ubiquinones. The slight differences between these numbers and 12,110 (or 6055) are due to a few bypasses (see below) and to those redox centres which remained reduced (with one electron) at the end of the simulation. It is clear that the number of non-return electron transfers is much lower than the total number of electron transfers to any of the reduced centres. For instance, up to 85,272,945 electrons go to the N4 centre. This means that each electron passes more than 7000 times through this redox centre on average. In other words, the electrons do not go directly from NADH to Q, but spend most of their time continuously flitting between the redox centres.

In addition, a few electrons do not follow the pathway formed by the redox centres in the structure of complex I (Fig. 1) but jump to another neighbouring centre. In the above simulation, a few electrons went directly from N1a to N3 (10 out of 998,521), from N3 to N5 (3 out of 74,030,852) and from N5 to N6b (1 out of 812,155,530). We also counted 14 electron transfers from N4 to N7. Because of the large distance between N4 and N7 and since N4 is reduced most of the time, the probability that this electron will return is low so N7 remains reduced most of the time. However with parameter set #2, the reduction in N7 decreases due to the fact that now N4 is less reduced. Nevertheless, in our simulations N7 does not seem to be involved in the catalytic process, in agreement with the literature [22,35].

To evaluate the role of the redox centres N1a and N2, we performed simulations with the two parameter sets in Table 1 for which these centres have different midpoint potentials (see also Fig. 2). In addition a simulation was run in the absence of N1a (with the parameter set #1) in order to better understand its role. The results are presented in Table 4 which gives the percentage of reduction of each redox centre. This percentage is calculated by dividing the sum of time intervals during which a centre is reduced, by the total length of the simulation. In all simulations the rate is around $610\ s^{-1}$. It appears that the redox centres are rather reduced (generally>50%) except for N3, N4, N5 with parameter set #2 (due to their slightly lower midpoint potential) and above all for N1a in the parameter set #1 (<9%).

In both cases, N2 is highly reduced, particularly with parameter set #1, owing to its high midpoint potential. This is accompanied by a decrease in the residence time of SQ• species (1.6% instead of 4.9%). This shows a possible role of N2 to decrease the presence of SQ• species depending of its midpoint potential.

More generally, the residence time of the semiquinone species FMNH• and SQ• (potential ROS producers [54,55]) are rather low (1.6% – 4.4%). Interestingly, FMNH• residence time is lower in the presence of N1a than in its absence (5.4%). It has been proposed that N1a could play a transient electrons storage role by decreasing the residence time of the flavosemiquinone FMNH•. According to this hypothesis, both FMN electrons might pass almost simultaneously to N3 and N1a [26]. The results in Table 4 test this prediction and show that the situation is more complex and depends on the midpoint potential of N1a. A thorough analysis (Fig. 4) of the electron transfers from $FMNH_2$ and FMNH• to N1a and N3 shows that less than 1.7% of the $FMNH_2$ or FMNH• electrons are transferred to N1a in all cases. This is particularly obvious with the parameter set #2 (0.2%) (Fig. 4C and D). The reason for that is the large distance between N1a and the FMN site (as compared with the distance of the FMN site to N3). This clearly shows that in both sets of parameters, N1a does not allow the quasi simultaneous transfer of both $FMNH_2$ electrons on N3 and N1a.

With parameter set #2 (Fig. 4C and D), while the electron transfer on N1a is lower (0.2%) than with set #1, the residence time of the electrons on N1a is paradoxically much higher (84.2% instead of 8.8%).

Table 3
Results of 10 s simulation with parameter set #1 for the reactions taking place within one single complex I molecule. Reoxidation of cytochrome QH_2 and reduction of NAD^+ formed are added to insure a steady-state flux in the complex. Non-return transfers are calculated by eliminating the forth and back electron movements.

Reduction of redox centres	Total electrons transfers to the centre	Non-return electron transfers
N1a	998521	4
N1b	6729268	11428
N3	74030852	12107
N4	85272945	12073
N5	81215530	12104
N6a	23774419	12102
N6b	24101225	12102
N2	561826	12101
N7	14	1
$FMNH_2$ => FMNH•	34850610	6055
FMNH• => FMN	37443751	6055
Q => SQ•	165484	6050
SQ• => QH_2	28063	6050

Table 4
Comparison of the redox states of the redox centres using the two parameter sets described in Table 1, and in the case of parameter set #1 in the absence of N1a. Each simulation is performed five times during 10 s. The bold data are the possible sensitive values for ROS production.

Redox centres	Parameter set #1	Parameter set #1 in absence of N1a	Parameter set #2
Turnover	$612 \pm 8\ s^{-1}$	$612 \pm 9\ s^{-1}$	$608 \pm 5\ s^{-1}$
	% reduction	% reduction	% reduction
N1a	**8.8** ± 0.5	–	**84.2** ± 0.6
N1b	68.4 ± 2.0	67.4 ± 1.5	64.6 ± 0.8
N3	68.5 ± 2.0	67.4 ± 1.5	44.6 ± 0.7
N4	68.4 ± 2.0	67.4 ± 1.5	34.4 ± 0.7
N5	68.4 ± 2.0	67.4 ± 1.5	34.4 ± 0.7
N6a	65.8 ± 2.0	64.8 ± 1.5	64.2 ± 0.8
N6b	65.8 ± 2.0	64.8 ± 1.5	64.2 ± 0.8
N2	**92.4** ± 0.8	**92.4** ± 1.0	**74.3** ± 0.8
N7	78.3 ± 3.8	75 ± 11	51.6 ± 4.6
$FMNH_2$	20.6 ± 1.3	19.8 ± 1.0	20.5 ± 0.8
FMNH•	**4.1** ± 0.1	**5.4** ± 0.8	**4.4** ± 0.1
NADH in active site	26.9 ± 1.6	26.9 ± 1.1	27.2 ± 1.0
QH_2 in active site	92.8 ± 0.8	92.6 ± 0.5	91.4 ± 0.5
SQ• in active site	**1.6** ± 0.2	**1.7** ± 0.2	**4.9** ± 0.3

Simultaneously the amount of FMNH• slightly increases (4.1% to 4.44%, Table 4). This low amount of electron transfer associated with a high level of electron residence on N1a in parameter set #2 is due to the high potential of N1a (-235 mV) which traps the electrons. Indeed at a much higher potential, only one electron would go to N1a and stay there. Thus, when one electron jumps to N1a, it remains there for some time, during which both electrons of the subsequent $FMNH_2$ molecules pass directly to N3 and the main flow of electrons. This situation is equivalent to the absence of N1a, a situation in which there was also an increase in FMNH•.

However, in parameter set #1, the electron on N1a is not trapped. Furthermore, the analysis of the net fluxes of electrons (Fig. 5) demonstrated a net positive electron flux from FMNH• to N1a associated with a quasi equivalent flux from N1a to a subsequent FMNH• giving $FMNH_2$. This provides two ways to slightly decrease the flavosemiquinone residence time (as compared to the absence of N1a).

In both parameter sets the presence of N1a slightly diminishes the lifetime of the flavosemiquinone FMNH•.

The reduction percentages of the redox centres we obtain (Table 4) are lower than those reported in the literature [56,57], even when we calculate them in the absence of products (Table 5). This observation can be linked with the higher k_{cat} we observe and could have several explanations: i) the distances between the redox centres are different in *E. coli* and much more different in beef heart from what is given by the crystal structure of the peripheral arm of *T. thermophilus*. ii) the K_d for substrates and products are not the correct ones. iii) we do not take into account the membranous arm of complex I, iv) the model is inaccurate. We discuss these points one by one.

i) It should be noticed that the results depend strongly upon the structure of the peripheral arm of complex I which is known for only one species [26,27] and on the midpoint potentials which seem different in bacteria and in mitochondria [41]. In other words we hypothesize that the position of the redox centre of complex I is the same whatever the species. At the moment there is no crystallographic justification of this hypothesis except that all species contain equivalent redox components [42]. Compared with the situation for bc_1 complex, it should be noted that for this latter complex several structures are known in different species, all of them showing redox centres which are perfectly superimposable from prokaryotes to eukaryotes. However this invariance in bc_1 complex cannot be taken as a proof of the existence of a similar invariance in complex I over different species.

ii) We estimated the rate constants of binding and release of the substrates and products. As explained in the Methods/model section we tried to find reasonable values in accordance with the known kinetic parameters (K_M, K_i). However, the latter are combinations of the rate constants and the knowledge of K_M and K_i does not imply a unique determination of the rate constants. We have reduced the affinity of Q by a factor of 10 and of NADH by a factor of 100 (separately in different simulations) without any change in the k_{cat} and in the reduced state of the redox centres (Table 5). An increase of K_d(Q) by a factor 100 does not significantly decrease the k_{cat} and moderately increases the reduction of the redox centres without reaching the observed values in these conditions. This demonstrates that these steps are probably not limiting except if they are decreased by a larger factor. The only way to both decrease the k_{cat} and to increase the reduction of the redox centres is to have, in the vicinity of the quinone binding site, a low concentration of Q and/or a high concentration of QH_2. It must be emphasized at this point that iii) in our simulations we only took into account the hydrophilic arm of complex I. The most obvious explanation for a slower k_{cat} particularly for bovine heart complex I is the fact that other steps certainly follow the transfer of electrons from N2 to Q. Furthermore, a second quinone binding site has been described [8,12–14] which could well be in interaction with the quinone site close to N2 slowing down the whole process at steady state. Another point concerns a possible transconformation, a process which is usually slow (compared to electron transfers) [43,59]. Conformational changes have been described in complex I and are necessary to explain the coupling between electron transport and proton pumping (see discussion in [21]). Both processes could slow down the reoxidation of QH_2 in the vicinity of N2, leading to a local increase in QH_2 concentration. This local high QH_2 concentration would lead to an increase in the reduction percentage of the redox centres and to a decrease in the k_{cat}.

Finally we have iv) to question our model which is certainly at this stage a poor representation of reality due to the lack of knowledge particularly on the membranous arm of the complex.

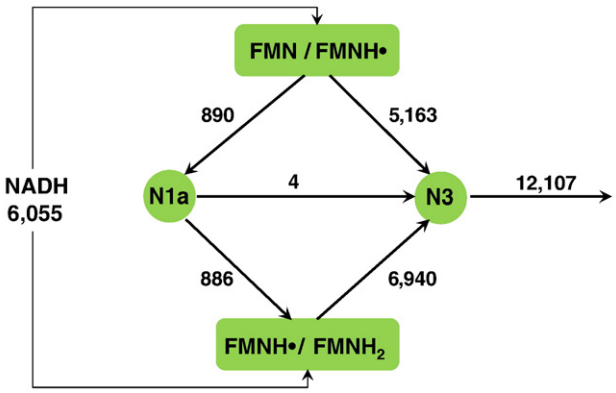

Fig. 5. Net electron flux in the triangle FMN – N1a – N3. The direction of the arrows indicates the direction of a positive net flux of electrons. The net number of electrons passing during the 10 s simulation is indicated along the arrows (parameter set #1). The FMN site is duplicated in order to describe the two possible redox reactions.

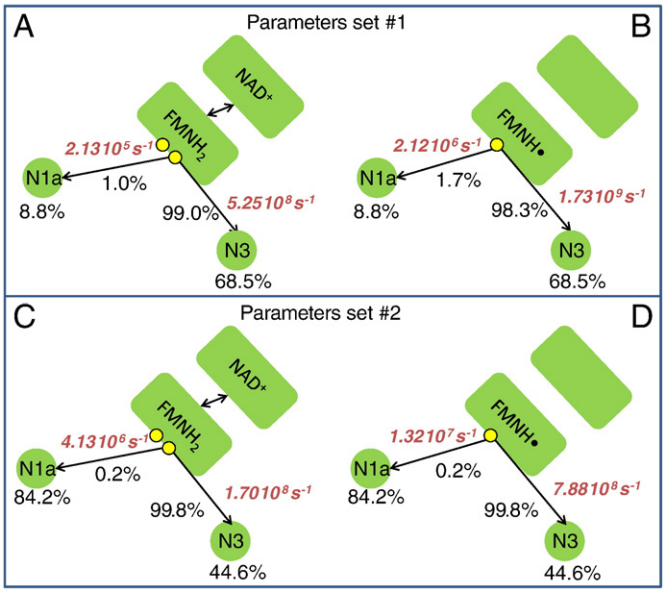

Fig. 4. Electrons transferred from FMN to N1a and N3 according to the two parameter sets used. Values under N1 or N3 represent the reduction percentage of the site at steady state. Other numbers along the arrows are rate constants (red italic) and the observed electron transfer in percent. They are calculated using the total number of electron exchanged between the redox centres, i.e. taking into account the unproductive to and fro electron transfers. ○ electron.

Table 5
Comparison of the reduced state of the redox centres as a function of the substrates affinity. Parameter set #1. Each simulation is performed during 1 s. Initial concentrations of [NADH] = [Q] = 16.6 mM (saturating values). No initial product concentration ([NAD+] = [QH_2] = 0).

Redox centres	parameter set #1 K_d NADH × 1 K_d Q × 1	parameter set #1 K_d NADH × 100 K_d Q × 1	parameter set #1 K_d NADH × 1 K_d Q × 10	parameter set #1 K_d NADH × 1 K_d Q × 100
	Mean of 10 simulations	Mean of 5 simulations	Mean of 5 simulations	Mean of 5 simulations
Turnover	$842 \pm 26\ s^{-1}$	$851 \pm 15\ s^{-1}$	$822 \pm 31\ s^{-1}$	$790 \pm 17\ s^{-1}$
	% reduction	% reduction	% reduction	% reduction
N1a	8.8 ± 3.0	7.7 ± 5.4	9.1 ± 2.4	13.8 ± 4.6
N1b	50.8 ± 5.7	50.5 ± 8.2	51.5 ± 3.8	65.4 ± 3.9
N3	50.9 ± 5.7	50.5 ± 8.2	51.6 ± 3.8	65.5 ± 3.9
N4	50.8 ± 5.7	50.5 ± 8.2	51.5 ± 3.8	65.4 ± 3.9
N5	50.8 ± 5.7	50.5 ± 8.2	51.5 ± 3.8	65.4 ± 3.9
N6a	47.3 ± 5.9	47.0 ± 8.0	48.0 ± 3.5	61.9 ± 3.9
N6b	47.2 ± 5.9	47.0 ± 8.0	48.0 ± 3.5	61.9 ± 3.9
N2	78.0 ± 6.6	81.2 ± 6.9	79.9 ± 4.7	88.4 ± 3.2
N7	51 ± 29	44 ± 36	77 ± 30	68 ± 32
$FMNH_2$	10.7 ± 2.7	14.5 ± 1.9	11.0 ± 1.5	17.3 ± 1.6
FMNH•	4.2 ± 1.3	3.6 ± 1.9	4.3 ± 1.1	6.4 ± 1.7
NADH in active site	15.1 ± 3.8	14.8 ± 6.3	15.6 ± 1.8	24.4 ± 1.9
QH_2 in active site	84.0 ± 2.8	83.9 ± 3.4	85.0 ± 2.1	91.3 ± 2.9
SQ• in active site	2.1 ± 0.9	2.8 ± 1.4	2.2 ± 0.7	1.4 ± 1.1

4. Conclusion

In summary, the stochastic approach to complex I functioning shows considerable continuous flitting to and fro of the electrons between nearly all the redox centres. However the net flux of electrons mainly follows the route defined by $NADH^+$ site – FMN – N3 – N1b – N4 – N5 – N6a – N6b – N2 – UQ site with a few exceptions.

The main exception concerns N1a, which does not appear to be a target receiving the second electron of $FMNH_2$, nearly simultaneously with the first electron to N3. Rather, when reduced, N1a functions as a repulsive centre for the subsequent electrons coming from $FMNH_2$, and orienting them towards N3. In addition, because N1a is mainly reduced from the FMNH• species and also oxidized by another FMNH•, it contributes to a slight decrease in the flavosemiquinone lifetime. We confirm the observation that the redox centres are largely reduced but cannot establish any special role for N7.

The high turnover number calculated in our simulations associated to non highly reduced redox centres is in contradiction with the observations and simply indicates that we are modelling only part of the mechanism of quinone reduction by complex I. It is the interest of a model to unveil these sorts of discrepancies between what is observed and what is calculated from observations at a lower level.

In the absence of a model, the data at the molecular level derived from the structure and the midpoint potentials on the one hand, and the kinetic results on the other hand, will stay apart from each other, although the latter derives clearly from the former.

Acknowledgements

We are indebted to R. Cooke for revising the English. This work was supported by a grant from ANR/BBSRC SysBio MitoScoP and by the “Ateliers epigenomic”, Genopole and University of Evry.

References

[1] J.E. Walker, The NADH:ubiquinone oxidoreductase (complex I) of respiratory chains, Q. Rev. Biophys. 25 (1992) 253–324.
[2] T. Friedrich, K. Steinmüller, H. Weiss, The proton-pumping respiratory complex I of bacteria and mitochondria and its homologue in chloroplasts, FEBS Lett. 367 (1995) 107–111.
[3] T. Friedrich, Complex I: a chimaera of a redox and conformation-driven proton pump? J. Bioenerg. Biomembr. 33 (2001) 169–177.
[4] U. Brandt, Energy convertin NADH:quinone oxidoreductase (Complex I), Ann. Rev. Biochem. 75 (2006) 69–92.
[5] J. Hirst, Towards the molecular mechanism of respiratory complex I, Biochem. J. 425 (2010) 327–339.
[6] U. Brandt, S. Kerscher, S. Dröse, K. Zwicker, V. Zickermann, Proton pumping by NADH:ubiquinone oxidoreductase. A redox driven conformational change mechanism? FEBS Lett. 545 (2003) 9–17.
[7] T. Yagi, A. Matsuno-Yagi, The proton-translocating NADH-quinone oxidoreductase in the respiratory chain: the secret unlocked, Biochemistry 42 (2003) 2266–2274.
[8] T. Ohnishi, Iron–sulfur clusters/semiquinones in complex I, Biochim. Biophys. Acta 1364 (1998) 186–206.
[9] S. Stolpe, T. Friedrich, The *Escherichia coli* NADH:ubiquinone oxidoreductase (complex I) is a primary proton pump but may be capable of secondary sodium antiport, J. Biol. Chem. 279 (2004) 18377–18383.
[10] J.M. Skehel, I.M. Fearnley, J.E. Walker, NADH:ubiquinone oxidoreductase from bovine heart mitochondria: sequence of a novel 17.2-kDa subunit, FEBS Lett. 438 (1998) 301–305.
[11] A. Chomyn, M.W.J. Cleeter, C.I. Ragan, M. Riley, R.F. Doolittle, G. Attardi, URF6, last unidentified reading frame of human mtDNA, codes for an NADH dehydrogenase subunit, Science 234 (1986) 614–618.
[12] A.D. Vinogradov, V.D. Sled, D.S. Burbaev, V.G. Grivennikova, I.A. Moroz, T. Ohnishi, Energy-dependent complex I-associated ubisemiquinones in submitochondrial particles, FEBS Lett. 370 (1995) 83–87.
[13] T. Ohnishi, J.E. Johnson Jr, T. Yano, R. LoBrutto, W.R. Widger, Thermodynamic and EPR studies of slowly relaxing ubisemiquinone species in the isolated bovine heart complex I, FEBS Lett. 579 (2005) 500–506.
[14] T. Ohnishi, J.C. Salerno, Conformation-driven and semiquinone-gated proton-pump mechanism in the NADHubiquinone oxidoreductase (complex I), FEBS Lett. 579 (2005) 4555–4561.
[15] Y. Hatefi, The mitochondrial electron transport and oxidative phosphorylation system, Annu. Rev. Biochem. 54 (1985) 1015–1069.
[16] U. Weidner, S. Geier, A. Ptock, T. Friedrich, H. Leif, H. Weiss, The gene locus of the proton-translocating NADH:ubiquinone oxidoreductase in Escherichia coli: organization of the 14 genes and relationship between the derived proteins and subunits of mitochondrial complex I, J. Mol. Biol. 233 (1993) 109–122.
[17] T. Yagi, T. Yano, S. Di Bernardo, A. Matsuno-Yagi, Procaryotic complex I (NDH-1), an overview, Biochim. Biophys. Acta 1364 (1998) 125–133.
[18] R. Hedderich Energy-converting, [NiFe] hydrogenases from Archaea and extremophiles: ancestors of complex I, J. Bioenerg. Biomembr. 36 (2004) 65–75.
[19] N. Grigorieff, Structure of the respiratory NADH:ubiquinone oxidoreductase (complex I), Curr. Opin. Struct. Biol. 9 (1999) 476–483.
[20] T. Friedrich, B. Böttcher, The gross structure of the respiratory complex I: a Lego System, Biochim. Biophys. Acta 1608 (2004) 1–9.
[21] V. Zickermann, S. Dröse, M.A. Tocilescu, K. Zwicker, S. Kerscher, U. Brandt, Challenges in elucidating structure and mechanism of proton pumping NADH: ubiquinone oxidoredictase (complex I), J. Bioenerg. Biomembr 40 (2008) 475–483.
[22] V. Zickermann, S. Kerscher, K. Zwicker, M.A. Tocilescu, M. Radermacher, U. Brandt, Architecture of complex I and its implications for electron transfer and proton pumping, Biochim. Biophys. Acta 1787 (2009) 574–583.
[23] G. Hofhaus, H. Weiss, K. Leonard, Electron microscopic analysis of the peripheral and membrane parts of mitochondrial NADH dehydrogenase (complex I), J. Mol. Biol. 221 (1991) 1027–1043.
[24] G. Tuschen, U. Sackmann, U. Nehls, H. Haiker, G. Buse, H. Weiss, Assembly of NADH:Ubiquinone reductase (complex I) in Neurospora mitochondria: independent pathways of nuclear-encoded and mitochondrially encoded subunits, J. Mol. Biol. 213 (1990) 845–857.

[25] T. Friedrich, D. Scheide, The repiratory complex I of bacteria, archea and eukarya and its module common with membrane-bound multisubunit hydrogenases, FEBS Lett. 479 (2000) 1–5.
[26] L.A. Sazanov, P. Hinchliffe, Structure of the hydrophilic domain of respiratory complex I from *Thermus thermophilus*, Science 311 (2006) 1430–1436.
[27] J.M. Berrisford, L.A. Sazanov, Structural basis for the mechanism of respiratory complex I, JBC 284 (2009) 29773–29783.
[28] V.D. Sled, N.I. Rudnitzky, Y. Hatefi, T. Ohnishi, Thermodynamic analysis of flavin in mitochondrial NADH: ubiquinone oxidoreductase (complex I), Biochemistry 33 (1994) 10069–10075.
[29] C.C. Moser, T.A. Farid, S.E. Chobot, P.L. Dutton, Electron tunneling chains of mitochondria, Biochim. Biophys. Acta 1757 (2006) 1096–1109.
[30] D. Flemming, S. Stolpe, D. Schneider, P. Hellwig, T. Friedrich, A possible role for iron–sulfur cluster N2 in proton translocation by the NADH:ubiquinone oxidoreductase (complex I), J. Mol. Microbiol. Biotechnol. 10 (2005) 208–222.
[31] G. Yakovlev, T. Reda, J. Hirst, Reevaluating the relationship between EPR spectra and enzyme structure for the iron–sulfur clusters in NADH:quinone oxidoreductase, Proc. Natl. Acad. Sci. 104 (2007) 12720–12725.
[32] T. Friedrich, B. Böttcher, The gross structure of the respiratory complex I: a Lego System, Biochim. Biophys. Acta 1608 (2004) 1–9.
[33] K. Zwicker, A. Galkin, S. Dröse, L. Grgic, S. Kerscher, U. Brandt, The Redox–Bohr group associated with iron–sulfur cluster N2 of complex I, J. Biol. Chem. 281 (2006) 23013–23017.
[34] T. Friedrich, The NADH:ubiquinone oxidoreductase (complex I) from *Escherichia coli*, Biochim. Biophys. Acta 1364 (1998) 134–146.
[35] T. Pohl, T. Bauer, K. Dörner, S. Stolpe, P. Sell, G. Zocher, T. Friedrich, Iron–sulfur cluster N7 of the NADH:ubiquinone oxidoreductase (Complex I) is essential for stability but not involved in electron transfer, Biochemistry 46 (2007) 6588–6596.
[36] C.C. Moser, T.A. Farid, S.E. Chabot, P.L. Dutton, Electron tunneling chains of mitochondria, Biochim. Biophys. Acta 1757 (2006) 1096–1109.
[37] S. Ransac, N. Parisey, J.-P. Mazat, The loneliness of the electrons in the *bc1* complex, Biochim. Biophys. Acta 1777 (2008) 1053–1059.
[38] C.C. Moser, C.C. Page, P.L. Dutton, Darwin at the molecular, Philos. Trans. R. Soc. B 361 (2006) 1295–1305.
[39] C.C. Moser, J.M. Keste, K. Warncke, R.S. Farid, P.L. Dutton, Nature of biological electron transfer, Nature 355 (1992) 796–802.
[40] P.L. Dutton, C.C. Moser, V.D. Sled, F. Daldal, T. Ohnishi, A reductant-induced oxidation mechanism for Complex I, Biochim. Biophys. Acta 1364 (1998) 245–257.
[41] L. Euro, D.A. Bloch, M. Wikström, M.I. Verkhovsky, M. Vershovskaya, Electrostatic interactions between FeS clusters in NADH:Ubiquinone Oxidoreductase (Complex I) from *Escherichia coli*, Biochemistry 47 (2008) 3185–3193.
[42] T. Ohnishi, E. Nakamaru-Ogiso, Were there any "misssignments" among iron–sulfur clusters N4, N5 and N6b in NADH-quinone oxidoreductase (Complex I)? Biochim. Biophys. Acta 1777 (2008) 703–710.
[43] A.D. Vinogradov, NADH/NAD + interaction with NADH:Ubiquinone oxidoreductase (complex I), Biochim. Biophys. Acta 1777 (2008) 729–734.
[44] G.C. Brown, M.D. Brand, Thermodynamic control of electron flux through mitochondrial cytochrome bc_1 complex, Biochem. J. 225 (1985) 399–405.
[45] M.P. Murphy, M.D. Brand, The control of electron flux through cytochrome oxidase, Biochem. J. 243 (1987) 499–505.
[46] H. Schägger, R. de Coo, M.F. Bauer, S. Hofmann, C. Godinot, U. Brandt, Significance of respirasomes for the assembly/stability of human respiratory chain complex I, J. Biol. Chem. 279 (2004) 36349–36353.
[47] G. Benard, B. Faustin, E. Passerieux, A. Galinier, C. Rocher, N. Bellance, J.-P. Delage, L. Casteilla, T. Letellier, R. Rossignol, Physiological diversity of mitochondrial oxidative phosphorylation, Am. J. Physiol. Cell Physiol. 291 (2006) 1172–1182.
[48] M.D. Esposti, Inhibitors of NADH-ubiquinone reductase: an overview, Biochim. Biophys. Acta 1364 (1998) 222–235.
[49] H.U. Bergmeyer, in: D.H. Williamson, J.T. Brosnan (Eds.), Methods of Enzymatic Analysis, Concentrations of Metabolites in Animal Tissues, vol. 4, Verlag Chemie International, 1974.
[50] D. Garfinkel, Simulation of the Krebs cycle and closely related metabolism in perfused Rat Liver. I. Construction of a Model, Comput. Biomed. Res. 4 (1971) 1–17.
[51] D.T. Gillespie, Exact stochastic simulation of coupled chemical reactions, J. Phys. Chem. 8 (1977) 2340–2361.
[52] M.L. Verkovskaya, N. Belevich, L. Euro, M. Wikström, M.I. Verkhovsky, Real-time electron transfer in respiratory complex I, Proc. Nat. Acad. Sci. U. S. A. 105 (2008) 3763–3767.
[53] A. Andreani, M. Granaiola, A. Leoni, A. Locatelli, R. Morigi, M. Rambaldi, M. Recanatini, G. Lenaz, R. Fato, C. Bergamini, Effects of new ubiquinone-imidazo[2, 1-b]thiazoles on mitochondrial complex I (NADH-ubiquinone reductase) and on mitochondrial permeability transition pore, Bioorg. Med. Chem. 12 (2004) 5525–5532.
[54] I. Fridovich, The biology of oxygen radicals, Science 201 (1978) 875–880.
[55] J.F. Turrens, Mitochondrial formation of reactive oxygen species, J. Physiol. 552.2 (2003) 335–344.
[56] G. Krishnamoorthy, P.C. Hinkle, Studies on the electron transfer pathway, topography of iron–sulfur centers, and site of coupling in NADH-Q oxidoreductase, J. Biol. Chem. 263 (1988) 17566–17575.
[57] A.B. Kotlyar, V.D. Sled, D.Sh. Burbaev, I.A. Moroz, A.D. Vinogradov, Coupling site I and the rotenone-sensitive ubisemiquinone in tightly coupled submitochondrial particles, FEBS Lett. 264 (1990) 17–20.
[58] T. Yano, W.R. Dunham, T. Ohnishi, Characterization of the $\Delta\mu_H+$-sensitive ubisemiquinone species (SQ_{Nf}) and the interaction with cluster N2: new insight into the energy-coupled electron transfer in complex I, Biochemistry 44 (2005) 1744–1754.
[59] A.D. Vinogradov, Catalytic properties of the mitochondrial NADH–ubiquinone oxidoreductase_(Complex I) and the pseudo-reversible active/inactive enzyme transition, Biochim. Biophys. Acta 1364 (1998) 169–185.